symmetry

MDPI

Article

A Novel Optical Path for Enhancing the Performance of High-Power Semiconductor Laser in Packaging

Chuanwu Liao [1], Xiaochuan Xia [1,*], Xiaofei Yang [2], Liang Zhang [3] and Guotong Du [1]

[1] School of Microelectronics, Dalian University of Technology, Dalian 116024, China
[2] School of Optoelectronic Science and Engineering, Collaborative Innovation Center of Suzhou Nano Science and Technology, Soochow University, Suzhou 215006, China
[3] Dalian Youopto Technology Co., Ltd., Dalian 116024, China
* Correspondence: xiaochuan@dlut.edu.cn; Tel.: +86-411-62273208

Abstract: High-power semiconductor laser has more significant applications in long distance and high-reliability optical communication systems. It is noticed that the packaging plays an important role in the performance of high-power semiconductor laser, including high output power, high coupling efficiency, low relative intensity noise (RIN), and so on. Usually, in a symmetrical optical path, the light, which incident directly parallel to the optical axis of the lens, will be partially reflected back to the laser and cause noise. To solve this problem, a novel asymmetric optical path is designed and implemented to meet the requirement of using a high-power laser with low RIN in this work. By employing an isolator between the first and second lens, the laser with high beam quality and low reflection of the signal was achieved. Moreover, the optical focal length of the collimating lens and the angle of the inclined lens were optimized by simulation. The proposed laser exhibited high coupling efficiency with a RIN of −168.89 dB/Hz. According to theoretical and experimental analysis, the performance of the laser will be helpful in fabricating a high-power laser with low RIN for next-generation optical communication.

Keywords: high-power laser; relative intensity noise; optical path; packaging

check for updates

Citation: Liao, C.; Xia, X.; Yang, X.; Zhang, L.; Du, G. A Novel Optical Path for Enhancing the Performance of High-Power Semiconductor Laser in Packaging. *Symmetry* **2022**, *14*, 1721. https://doi.org/10.3390/sym14081721

Academic Editor: Albert Ferrando

Received: 15 July 2022
Accepted: 14 August 2022
Published: 18 August 2022

Publisher's Note: MDPI stays neutral with regard to jurisdictional claims in published maps and institutional affiliations.

Copyright: © 2022 by the authors. Licensee MDPI, Basel, Switzerland. This article is an open access article distributed under the terms and conditions of the Creative Commons Attribution (CC BY) license (https://creativecommons.org/licenses/by/4.0/).

1. Introduction

In recent years, improving the speed of optical communication systems has increasingly been a requirement for developing high-power semiconductor lasers [1]. As demands on the performance of high-power semiconductor lasers increase, new packaging techniques must be developed to meet the demands for high power, high reliability, low relative intensity noise (RIN), and low cost. Numerous improvements such as soldering technique, thermal management, and optical output system have been made to the packing technology. It is worth noting that a single laser chip is the basic unit of a packaged high-power semiconductor laser. Furthermore, the RIN plays an important role in packaging technology, limiting the performance and reliability of high-power semiconductor lasers [2].

According to the working principle of a laser chip, the light emission of the laser chip is stimulated radiation [3]. Specifically, an electron in the excited state transitions a radiated photon to a lower energy or ground state, which possesses the same frequency, phase, propagation direction, and polarization state characteristics as external photons [4,5]. Unfortunately, due to the optical reflection, the emitted photons by stimulating radiation will introduce an extra system noise under the interference condition [6]. It was reported that the RIN value of a high-power laser is mostly controlled between −165 dB/Hz and −150 dB/Hz, which is unable to meet the standard requirements in 5G optical communication [7–11].

In this work, a novel packaging optical path for enhancing the performance of high-power semiconductor laser is proposed. An isolator is utilized to achieve high beam quality and low signal reflection. Moreover, the optical focal length of the collimating

lens and the angle of the inclined lens were optimized by simulation. The average RIN valve of −168.89 dB/Hz was obtained. Besides, the angle between the beam axis of the semiconductor laser chip and the lens axis is also demonstrated. This work provides a feasible path for realizing low RIN optical path design in the optical communication field, which is sufficient to meet the requirements of improving the system rate of the sixth-generation (6G) optical communication in the future.

2. Materials and Methods

2.1. Optical Path Design

The principle diagram of the double lens optical path of the optical transmitter is shown in Figure 1. The optical emission chip as the light source emits Gaussian light, which becomes parallel light after passing through the collimating lens, and converges into the optical fiber core after reaching the focusing lens through the isolator. Figure 2 displays the results of the simulation. It was found that coupling efficiency was 93.45% with 1550 nm. However, the optical centers of all components are on the same optical axis in this optical path system. This kind of coaxial optical system can induce extra RIN, and the RIN can only reach −150 dB/Hz. Simultaneously, the light from the chip is reflected onto the chip through subsequent optical elements, causing laser damage. In order to solve this problem, the optical system was optimized and simulated by ZEMAX software. Meanwhile, the evaluation function in ZEMAX was used to restrict some parameters, including the curvature radius of the lens, aspherical coefficient, material, etc. The coupling efficiency is guaranteed, and the back loss by the eccentricity of the light source or tilt of the lens is reduced. The setting parameters are shown in Table 1. The double lens optical path model after finish optimization is shown in Figure 3. It is observed that the eccentric distance of the light source along the x-axis direction is 50 μm, and the collimating lens is inclined by 3°. The proposed packaged single laser exhibited good RIN with a high coupling efficiency of 88.92%, shown in Figure 4.

Table 1. Setting Parameters of Zemax.

	Collimating lens		Focal lens	
Material	VCSEL-LENS		K-PBK40	
Mechanical half diameter/mm	0.275 mm		0.275 mm	
Aperture/mm	0.25 mm		0.275 mm	
Thickness/mm	0.72		1.1	
Focal length/mm	0.17		1.9	
Radius of curvature	0.754	−0.482	1.4	−8.632
Aspheric coefficient	−24.476	−1.079	−0.101	−74.471
Forth term coefficient	0.006406	−0.298	−0.017	0.017
Sixth term coefficient	−0.192	0.519	−0.001632	0.028
Eighth term coefficient	/	0.891	−0.002056	−0.018
Tenth term coefficient	/	1.532	−3.025	/

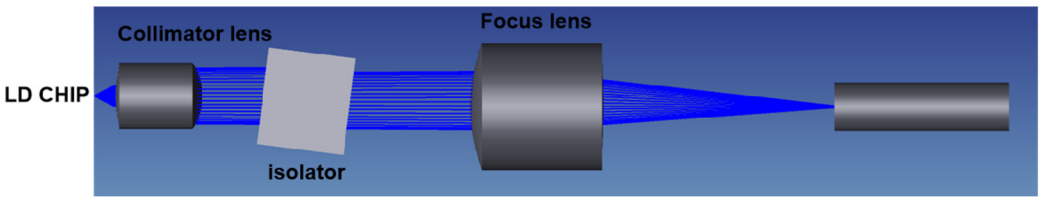
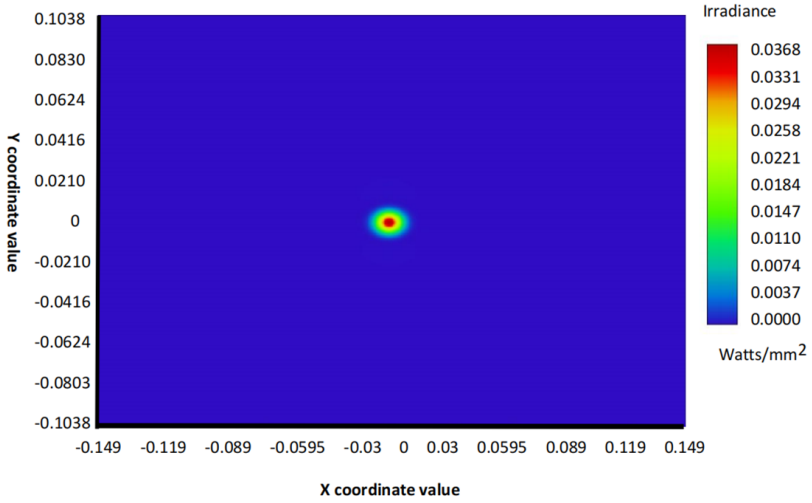


Figure 1. Ideal optical path model of high-power laser.



Total Irradiance surface 22 fiber end

grin

2022/8/3

Wavelength 1.55000 µm in index 1.44402 at 0.0000 mm

Display X Width = 2.9763×10^{-1}, Y Height = 2.0795×10^{-1} Millimeters

Peak Irradiance =3.6803×10^{-2} Watts/Millimeters^2 , Total Power = 2.8017×10^{-6} Watts

Fiber Efficiency : System 0.995582 , Receiver 0.938683, Coupling 0.934537

Figure 2. Coupling efficiency simulation of Ideal optical path model.

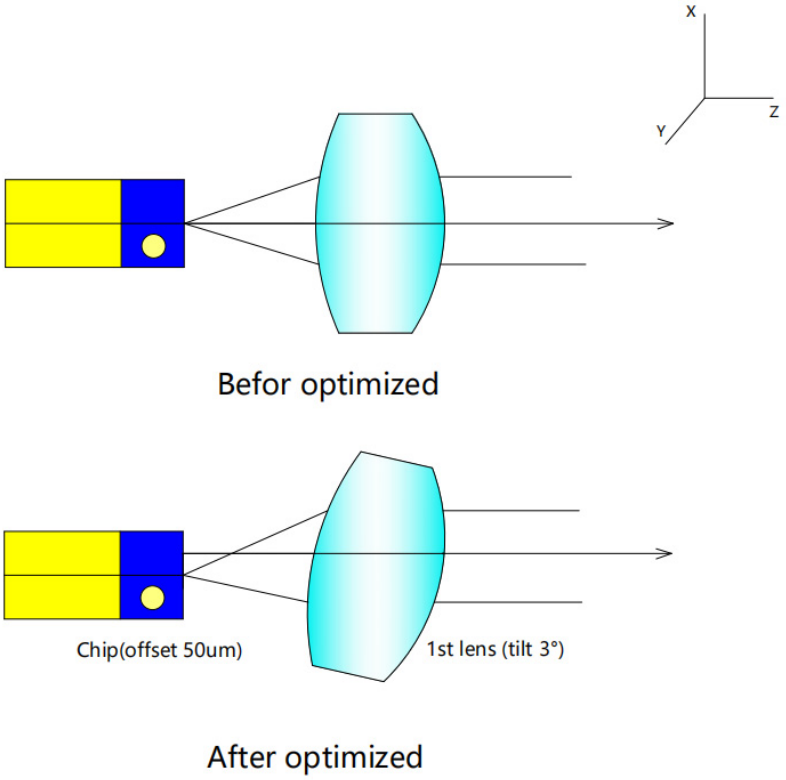
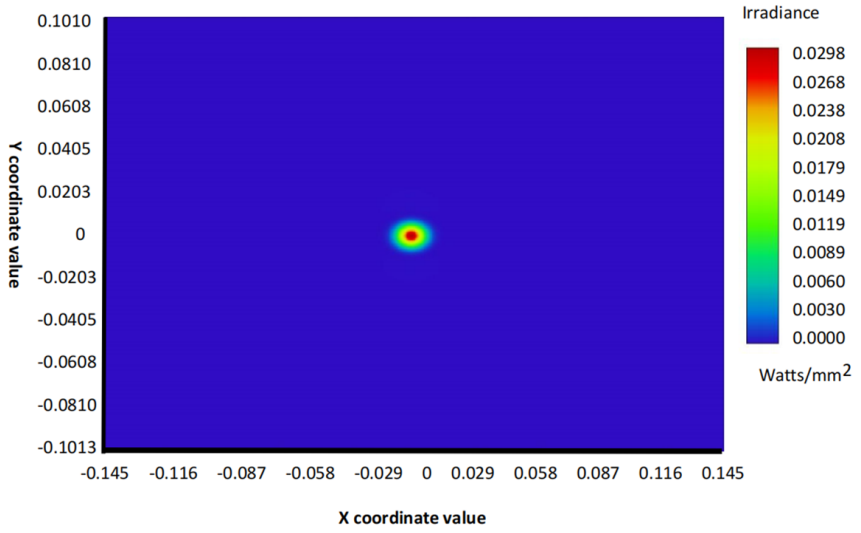


Figure 3. Optical path model after finish optimization.



Total Irradiance surface 22 fiber end

grin

2022/8/3

Wavelength 1.55000 μm in index 1.44402 at 0.0000 mm

Display X Width = 2.8999×10^{-1}, Y Height = 2.0261×10^{-1} Millimeters

Peak Irradiance = 2.9766×10^{-2} Watts/Millimeters^2 , Total Power = 2.804×10^{-6} Watts

Fiber Efficiency : System 0.996407 , Receiver 0.902524, Coupling 0.899281

Figure 4. Coupling efficiency simulation of an optimized optical path model.

2.2. Device Assembly

The optical path of the optical device proposed in this paper requires optical components such as a lens and isolator to form a certain offset with the laser chip. High precision die bonder and multidimensional active optical path coupling system are needed in the assembly process. Firstly, the position of the laser chip is fixed with a die bonder with an accuracy of 5 μm. This position is the result of an optical strategy optimization. Secondly, the first lens was coupled using a multidimensional active optical path coupling system. By adjusting the position of the first lens, there is a minimum light spot on the mode field analyzer, as Figure 5 shown. Meanwhile, the position change of the light spot at 1000 mm is less than 500 μm. Then the isolator was placed according to the same principle of placing the first lens. In the process of placing the isolator, it is necessary to ensure that the optical path insertion loss should be less than 0.3 dB. Finally, a second lens was placed according to the designed position to couple the light into the optical fiber, which can ensure the coupling efficiency above 85%.

These results indicated that the high coupling efficiency of above 80% could be achieved through fine-tuning the optical elements to make the laser chip offset along the x-axis direction and rotating the tilt angle of the collimating lens to realize low RIN. At the same time, the eccentricity can reach 50 μm, and the angle rotation can be greater than 1.8°. During the adjustment, eight dimensions (x_1,x_2,y_1,y_2,z,θ_x,θ_y,θ_z, xyz are axial motion, θ is angle motion) are required to adjust with a step accuracy greater than 0.5 μm.

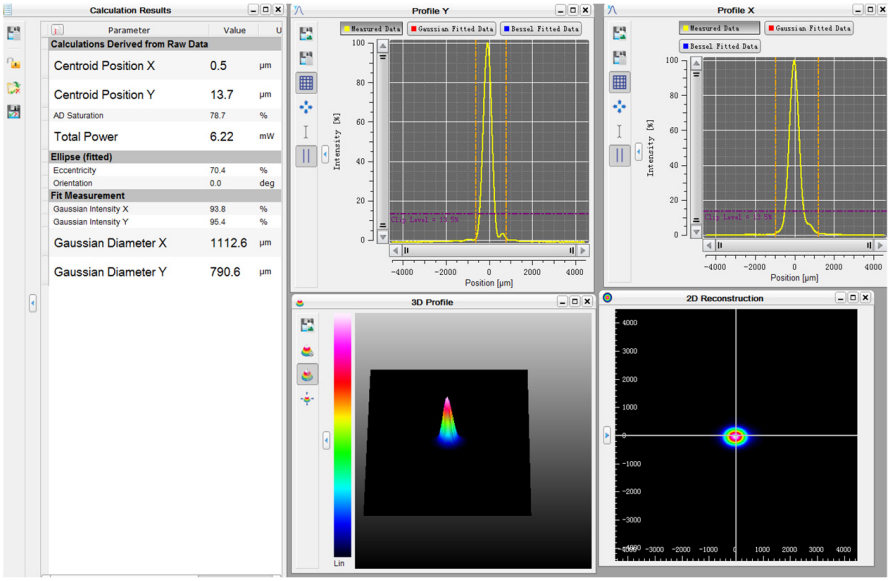


Figure 5. Measurement of laser spot after laser chip collimation with beam scan.

3. Results and Discussion

3.1. Theoretical Analysis

Most high-power laser adopts a dual-lens structure because of its high coupling efficiency [12,13]. The coupling efficiency of dual-lens structure simulation can reach more than 95%, but the coupling efficiency achieved by the actual process can only reach 80%. The coupling efficiency of single lens structure simulation is only 85%, and the coupling efficiency achieved by the actual process is only 65% [14]. The ideal optical path is shown in Figure 1. The light emitted by the laser chip passes through the first collimator lens to become parallel light and then passes through the second lens to converge into the optical fiber.

The output beam of the semiconductor laser is a paraxial wave, and the energy of the beam gradually diverges along the axis z direction, which is distributed as a Gaussian beam [15]. The change of Gaussian beam $\omega(z)$ with the axial distance z is shown in Figure 6. At $z = 0$, the beam width of $\omega(0) = \omega_0$ is the smallest, which is called the beam waist position. At $z = \pm z_0$, $\omega(\pm z_0) = \omega_0$, $\ln/z/ \geq z_0$, $\omega(z)$ changes linearly with z: $\omega(z) = z$, at this point, the equal phase surface is approximately spherical [16]. The optical field distribution of semiconductor laser is usually described by the near field and far field properties. The range of $z = \pm z$ is called the Rayleigh range of the Gaussian beam, and the near-field region refers to the region between the beam waist and Rayleigh length, and the region of $z > z_0$ is called the far-field region [17].

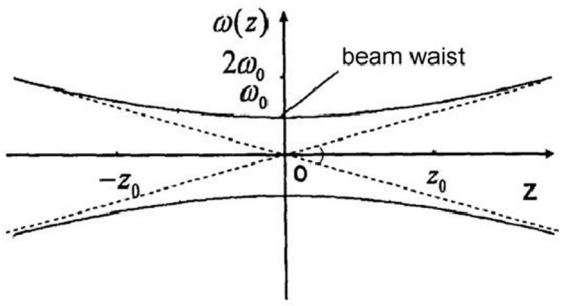


Figure 6. Schematic of Gaussian beam radius.

In order to improve the beam quality and reduce the impact of reflection on the signal, an isolator between the first and second lens is placed. The purpose is to prevent the light

passing through the isolator from reflecting the original path into the chip. The generated spontaneous radiation will affect the beam quality. The working principle of the isolator for the incident and reflected light beam is shown in Figure 7. The isolator consists of three parts: one 0° polarizer and two 45° polarizers. During the assembly of the isolator, the position of the 0° polarizer should be consistent with the polarization direction of the laser chip, so the light emitted by the laser chip can pass through the 0° polarizer without loss, as shown in Figure 7a. The 45° polarizer rotates the polarization direction of the laser light to 45° and then passes through the 45° polarizer. In other words, the beam passes through the isolator and changes from horizontal polarization to 45° polarization. After passing through the isolator, the reflected light beam will change from 45° polarization to 90° polarization, which is exactly perpendicular to the direction of the 0° polarizer, thus preventing the light beam from injecting into the laser chip, as shown in Figure 7b. The isolation of the isolator needs more than 50 dB, and the insertion loss needs less than 0.3 dB. For example, as in Figure 8, the laser output power P1 is 10 dBm (100 mW); after passing through, the power Pmin will be 9.7 dBm. On the other side, if 2% (100 mW × 2% = 2 mW = 3.01 dBm) power was reflected as P2. the remaining power Pmax should be less than −46.99 dBm.

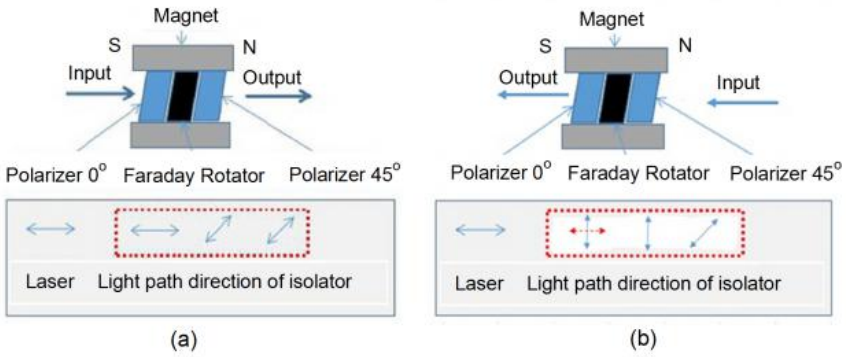


Figure 7. Working principle of the isolator (**a**) output light path (**b**) feedback light path.

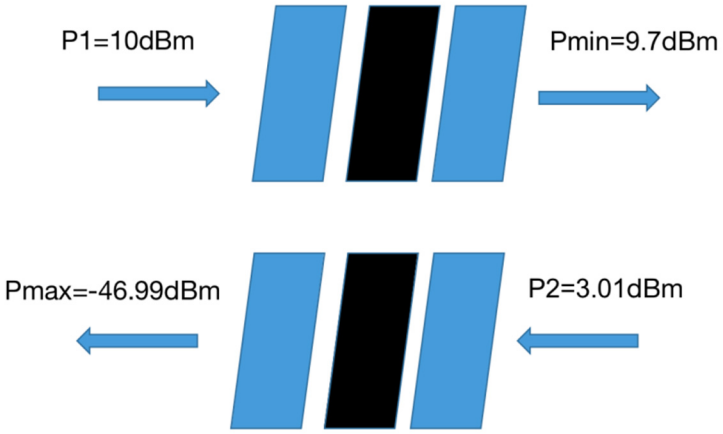


Figure 8. Output power through isolator.

3.2. Packaging and Testing

The light path of the 100 mw laser chip package after collimating the light spot is shown in Figure 4. The light quality meets the design requirements through the collimator lens. The beam analyzer measured the spot position at 10 cm and 100 cm, and the spot center deviation was less than 0.5 mm. The Gaussian beam can be acquired using the following equation [18]

$$E = E_0 \frac{W_0}{W(z)} \exp\left(-\frac{r^2}{W^2(z)}\right) \quad (1)$$

where z is the distance propagated from the plane when the wavefront is flat, W_0 is the radius of the irradiance contour at the plane, and $W(z)$ is the radius of the $1/e^2$ contour after the wave has propagated a distance z. When the amplitude has fallen to $1/e^2$ of the maximum value within the beam section, the distance from the optical axis is defined as the spot radius.

$$r = W(z) \tag{2}$$

From the definition of $W(z)$, we can get:

$$\frac{W^2(z)}{{W_0}^2} - \frac{z^2}{{z_0}^2} = 1 \tag{3}$$

The calculated change ratio of 10 cm collimation spot diameter and 100 cm spot diameter was less than 0.005, and the actual change ratio of spot diameter was 0.003. The optical fiber welding process was carried out after packaging the second lens. Finally, the fiber input power of the laser was measured to be 81 mW, that is, the packaging coupling efficiency reached 80%. Meanwhile, testing the RIN performance by using the system is shown in Figure 9. PD device was needed to transform the optical signal into an electronic signal; the signal analyzer can conclude the relative intensity noise of this laser. It can be observed in Figure 10 that the RIN of the laser is still very high, even at high coupling efficiency. Meanwhile, there was a strong feedback signal at around 2.8 GHz.

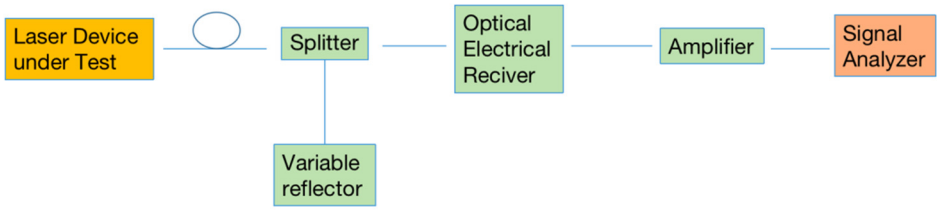


Figure 9. RIN test system.

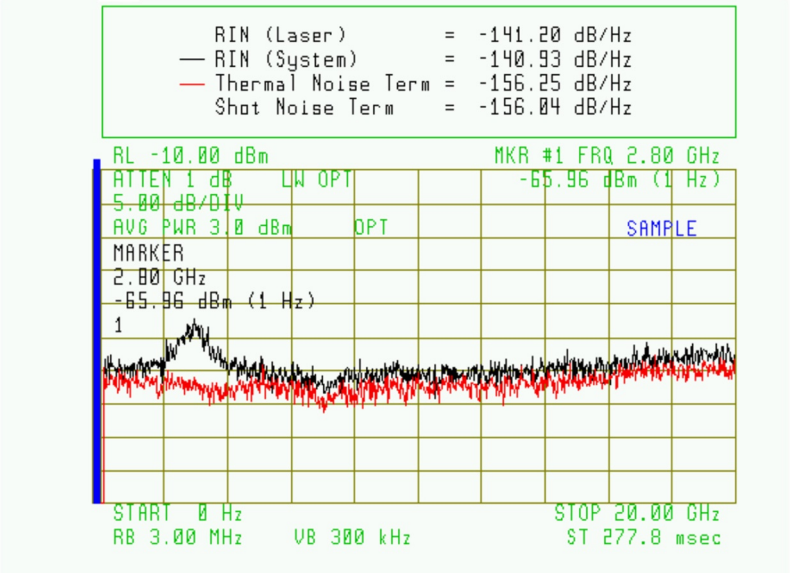


Figure 10. Relative intensity noise test of laser.

3.3. Optimization and Test of Optical Path Reflection

It is very difficult to achieve a coupling efficiency of 80% based on the actual process level, but only 20% of the light energy is reflected. At present, most high-power laser chips are directly modulated laser (DML) chips, so the influence of the 20% optical path reflection is very serious. How to avoid the reflected light from affecting the laser chip is the main

point of the design. Figure 11 shows the optical path model for lenses near focus and with partial focus. Defocusing between chip and lens is unavoidable in the actual packaging process. Defocusing will cause the reflected light to enter the laser chip region, which will interfere with the laser chip's luminescence and generate noise, as shown in Figure 12a. The laser region diameter of the laser chip is generally about 2 µm. The effective way to ensure the coupling efficiency is to make the lens and chip at a 3° angle; this design can avoid reflected light entering the active region, as shown in Figure 12b.

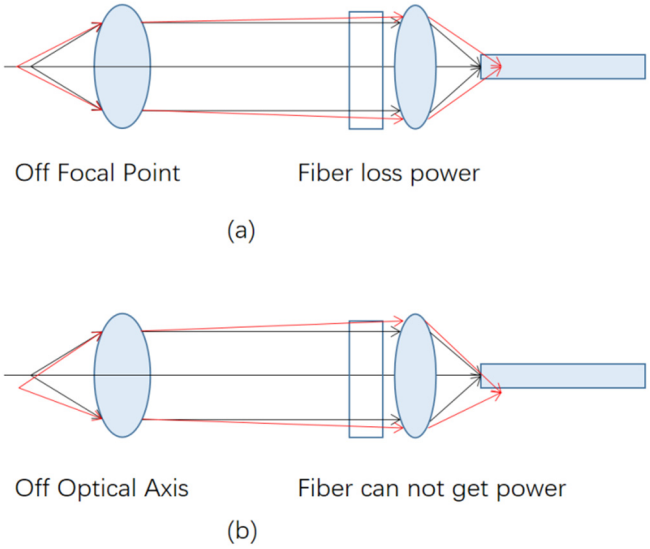


Figure 11. Actual optical path model of laser (**a**) lens near focus (**b**) lens with partial focus.

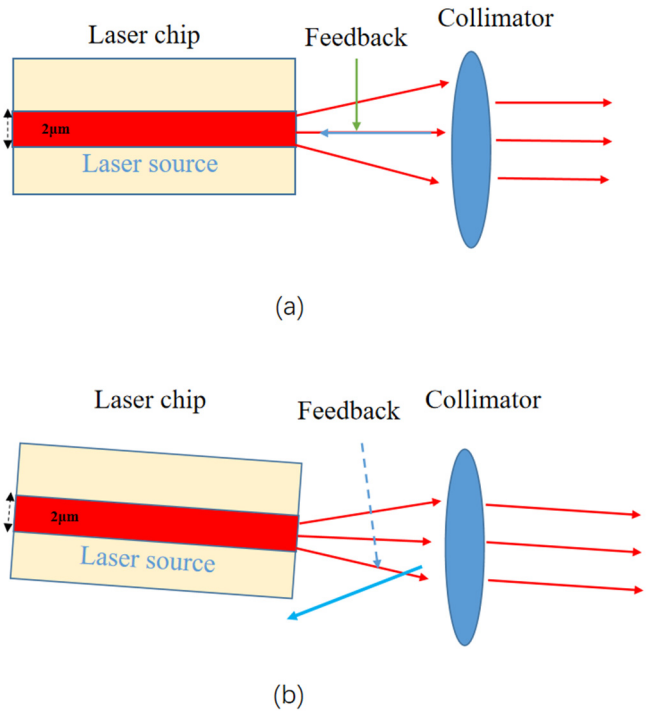


Figure 12. Schematic diagram of laser beam and feedback between laser chip and collimation lens (**a**) laser chip and collimator lens without angle (**b**) laser chip and collimator lens with angle.

Using software simulation, it has been found that lengthening the focal length of the collimating lens can achieve higher coupling efficiency and lower laser region reflection. When the collimating lens is generally at a distance of about 0.2 mm, some reflected light can still enter the chip. The optical path of the lens is shown in Figure 13. When the focal

length is about 0.6 mm, it can be seen that it is more challenging for the reflected light to enter the chip. After optimization, the theoretical coupling efficiency can reach more than 92%.

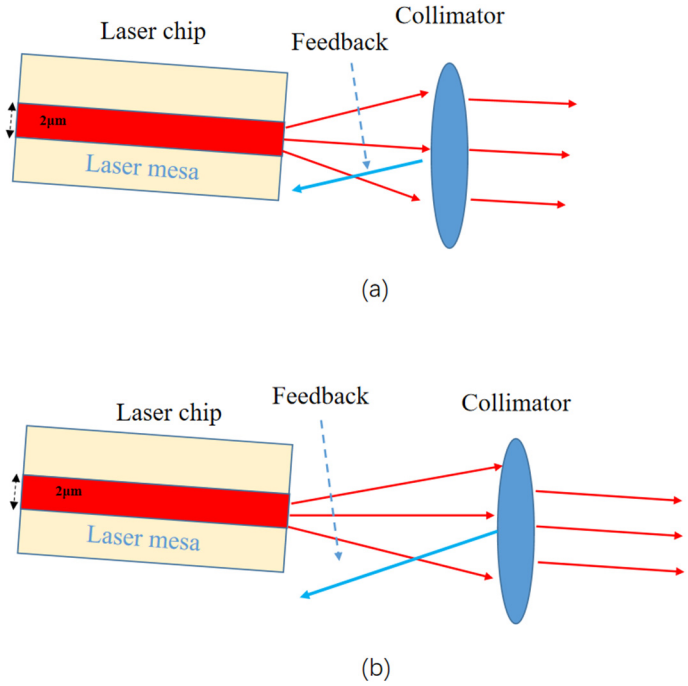


Figure 13. Schematic diagram of the laser beam and feedback with longer work distance collimation lens (**a**) short work distance (**b**) long work distance.

From the above theoretical analysis, the practical packaging experiments were conducted, and the coupling efficiency measured in practice was still up to 80%, which was the same as the previous coupling efficiency. It can be seen in Figure 14 that the RIN of the laser is about −169 dB/Hz with good performance.

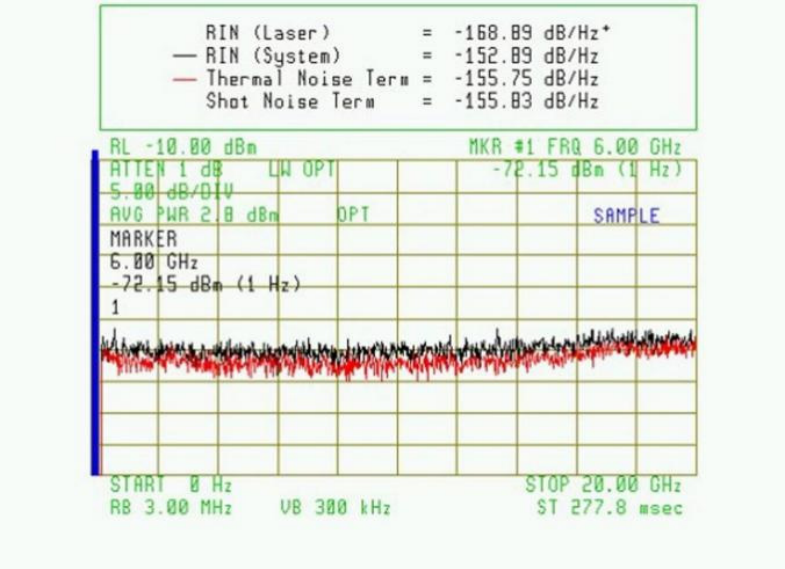


Figure 14. RIN test result of high-power laser after optimization.

4. Conclusions

Although the coupling efficiency of the optical path during laser assembling is improved, about 20% of the laser power can still be reflected. Some reflected power can enter the chip's laser region, causing serious interference. In this paper, an isolator is placed between the collimating lens and focus lens, which can ensure not only the optical coupling efficiency but also the influence of reflected laser power on the laser region of the chip. Furthermore, a longer working distance collimating lens is used in this optical system, as well as the chip and the collimating lens are placed at a small angle, which can decrease the effects of feedback simultaneously. The relative intensity noise of the device is improved from −141.2 dB/Hz to −168.89 dB/Hz, better than the reported RIN −165 dB/Hz. Consequently, the optical path will be used in high-power laser mass production. This improvement in laser RIN performance will accelerate the research in next-generation optical communication. In the following work, we will optimize the optical coating of the lens and other optical elements used in the laser device. The AR coating and HR coating would be added, which can increase the coupling efficiency and help reduce the reflection, respectively.

Author Contributions: Writing—original draft preparation and editing, C.L.; writing—review and editing, X.X.; data curation, X.Y.; validation, L.Z.; visualization, G.D. All authors have read and agreed to the published version of the manuscript.

Funding: This research received no external funding.

Institutional Review Board Statement: Not applicable.

Informed Consent Statement: Not applicable.

Data Availability Statement: Not applicable.

Acknowledgments: This study was funded by the Department of Science & Technology of Liaoning Province.

Conflicts of Interest: The authors declare no conflict of interest.

References

1. Yap, M.J.; Cripe, J.; Mansell, G.L.; McRae, T.G.; Ward, R.L.; Slagmolen, B.J.J.; Heu, P.; Follman, D.; Cole, G.D.; Corbitt, T.; et al. Broadband reduction of quantum radiation pressure noise via squeezed light injection. *Nat. Photonics* **2020**, *14*, 19. [CrossRef]
2. Zhao, J.; Guiraud, G.; Pierre, C.; Floissat, F.; Casanova, A.; Hreibi, A.; Chaibi, W.; Traynor, N.; Boullet, J. High-power all-fiber ultra-low noise laser. *Appl. Phys. B-Laser O* **2018**, *124*, 114. [CrossRef]
3. Rizzelli, G.; Iqbal, M.A.; Gallazzi, F.; Rosa, P.; Tan, M.; Ania-Castañón, J.D.; Krzczanowicz, L.; Corredera, P.; Phillips, I.; Forysiak, W.; et al. Impact of input FBG reflectivity and forward pump power on RIN transfer in ultralong Raman laser amplifiers. *Opt. Express* **2016**, *24*, 29170. [CrossRef]
4. Sheikhey, M.M.; Goudarzi, M.; Yadipour, R.; Baghban, H. Analytical investigation of relative intensity noise properties of injection-locked mid-IR quantum cascade lasers. *J. Opt. Soc. Am. B* **2016**, *33*, D57. [CrossRef]
5. Cheng, X.; Pan, W.W.; Zeng, X.; Dong, J.Y.; Cui, S.Z.; Feng, Y. Relative intensity noise comparison of fiber laser and amplified spontaneous emission sources. *Opt. Fiber Technol.* **2020**, *54*, 102119. [CrossRef]
6. Faugeron, M.; Tran, M.; Parillaud, O.; Chtioui, M.; Robert, Y.; Vinet, E.; Enard, A.; Jacquet, J.; van Dijk, F. High-Power Tunable Dilute Mode DFB Laser with Low RIN and Narrow Linewidth. *IEEE Photonic Technol. Lett.* **2013**, *25*, 7. [CrossRef]
7. Dicke, R.H. Coherence in Spontaneous Radiation Processes. *Phys. Rev.* **1954**, *93*, 99. [CrossRef]
8. Dudetskiy, V.Y.; Lariontsev, E.G.; Chekina, S.N. Synchronisation and desynchronisation of self-modulation oscillations in a ring chip laser under the action of a periodic signal and noise. *Quantum Electron.* **2014**, *44*, 806. [CrossRef]
9. Shi, J.X.; Qin, L.; Liu, Y.; Zhang, N.; Zhang, J.; Zhang, L.S.; Jia, P.; Ning, Y.Q.; Zeng, Y.G.; Zhang, J.L.; et al. Emission characteristics of surface second-order metal grating distributed feedback semiconductor lasers. *Chin. Sci. Bull.* **2012**, *57*, 2083. [CrossRef]
10. Morton, P.A. High-Power, Ultra-Low Noise Hybrid Lasers for Microwave Photonics and Optical Sensing. *J. Lightw. Technol.* **2018**, *36*, 5048. [CrossRef]
11. Gao, Y.K.; Lo, J.C.; Lee, S.; Patel, R.; Zhu, L.; Nee, J.; Tsou, D.; Carney, R.; Sun, J. High-Power, Narrow-Linewidth, Miniaturized Silicon Photonic Tunable Laser with Accurate Frequency Control. *J. Lightw. Technol.* **2020**, *38*, 265. [CrossRef]
12. Li, R.; Fan, W.; Jiang, Y.; Qiao, Z.; Zhang, P.; Lin, Z. Tunable compensation of GVD-induced FM–AM conversion in the front end of high-power lasers. *Appl. Opt.* **2017**, *56*, 993. [CrossRef] [PubMed]

13. Motaghiannezam, R.; Pham, T.; Chen, A.; Du, T.; Kocot, C.; Xu, J.; Huebner, B. 52 Gbps PAM4 receiver sensitivity study for 400GBase-LR8 system using directly modulated laser. *Opt. Express* **2016**, *24*, 7374. [CrossRef] [PubMed]
14. Wang, C.; Sun, J.; Sun, F.; Zhu, J.; Yuan, Z.; Asundi, A. Coupling efficiency of ultra-small gradient-index fiber probe. *Opt. Commun.* **2017**, *389*, 265. [CrossRef]
15. Tsai, J.H. Replacing the optical-lever method with the method using the spot radius of a laser beam to determine the curvature of a material. *Opt. Eng.* **2004**, *43*, 737. [CrossRef]
16. Zhang, T.; Wang, M.; Yang, Y.; Fan, F.; Lee, T.; Liu, H.; Xiang, D. An on-chip hybrid plasmonic light steering concentrator with ~96% coupling efficiency. *Nanoscale* **2018**, *10*, 5097. [CrossRef] [PubMed]
17. Zhai, T.; Tan, S.Y.; Lu, D.; Wang, W.; Zhang, R.K.; Ji, C. High Power 1060 nm Distributed Feedback Semiconductor Laser. *Chin. Phys. Lett.* **2014**, *31*, 024203. [CrossRef]
18. Liu, J.M. Simple technique for measurements of pulsed Gaussian-beam spot sizes. *Opt. Lett.* **1982**, *7*, 196. [CrossRef]